

# Cerebral White Matter Integrity Mediates Adult Age Differences in Cognitive Performance

David J. Madden<sup>1</sup>, Julia Spaniol<sup>1</sup>, Matthew C. Costello<sup>1</sup>,  
Barbara Bucur<sup>1</sup>, Leonard E. White<sup>1</sup>, Roberto Cabeza<sup>2</sup>, Simon W. Davis<sup>2</sup>,  
Nancy A. Dennis<sup>2</sup>, James M. Provenzale<sup>1</sup>, and Scott A. Huettel<sup>1</sup>

## Abstract

■ Previous research has established that age-related decline occurs in measures of cerebral white matter integrity, but the role of this decline in age-related cognitive changes is not clear. To conclude that white matter integrity has a mediating (causal) contribution, it is necessary to demonstrate that statistical control of the white matter–cognition relation reduces the magnitude of age–cognition relation. In this research, we tested the mediating role of white matter integrity, in the context of a task-switching paradigm involving word categorization. Participants were 20 healthy, community-dwelling older adults (60–85 years), and 20 younger adults (18–27 years). From diffusion tensor imaging tractography, we obtained fractional anisotropy (FA) as an index of white matter integrity in the genu and splenium of the corpus

callosum and the superior longitudinal fasciculus (SLF). Mean FA values exhibited age-related decline consistent with a decrease in white matter integrity. From a model of reaction time distributions, we obtained independent estimates of the decisional and nondecisional (perceptual–motor) components of task performance. Age-related decline was evident in both components. Critically, age differences in task performance were mediated by FA in two regions: the central portion of the genu, and splenium–parietal fibers in the right hemisphere. This relation held only for the decisional component and was not evident in the nondecisional component. This result is the first demonstration that the integrity of specific white matter tracts is a mediator of age-related changes in cognitive performance. ■

## INTRODUCTION

Neuroimaging studies have identified several forms of age-related change in brain structure that are relevant as potential mediators of age-related changes in cognitive performance. Prominent among these is age-related decline in the volume of cerebral gray matter, particularly in prefrontal regions (Raz, 2005; Raz et al., 2005; Resnick, Pham, Kraut, Zonderman, & Davatzikos, 2003; Tisserand et al., 2002). Age-related decline is also evident in cerebral white matter volume, although with a different trajectory. Whereas the age-related decline in gray matter volume is relatively linear from younger adulthood, the corresponding decline in white matter tends to be nonlinear, with a plateau in middle-age and additional decline, beyond that of gray matter, in later adulthood (Salat, Kaye, & Janowsky, 1999; Guttman et al., 1998; but cf. Marner, Nyengaard, Tang, & Pakkenberg, 2003).

Diffusion tensor imaging (DTI) can identify age-related changes in the microstructure of white matter that may not be detectable as a volumetric decline. This imaging modality is a form of MRI that measures both the rate and directionality of the displacement distribution of

water molecules across tissue components (Le Bihan, 2003; Basser & Jones, 2002; Beaulieu, 2002; Song, Wong, Tan, & Hyde, 1996). Diffusion can be described as occurring equally in all directions (isotropic) or restricted primarily to one direction (anisotropic). Diffusion tends to be more anisotropic in white matter than in gray matter due to many factors, such as the degree of compactness of white matter tracts, their myelination, and the number of axons within a specific region.

For each voxel, DTI estimates diffusion along multiple axes, typically separated into one major axis (eigenvector) of diffusion and two minor axes that are orthogonal to the primary eigenvector. The most frequently used measure of white matter integrity, fractional anisotropy (FA), is calculated on the basis of all three diffusivities (the eigenvalues  $\lambda_1$ ,  $\lambda_2$ ,  $\lambda_3$ ). The FA is a scalar measure (0–1.0) representing the relative directionality of diffusion, independent of its rate, with higher FA values representing a higher degree of directionality. Each eigenvalue represents the rate of diffusion, independent of directionality. DTI studies using animal models, confirmed by histology, have suggested that diffusivity parallel to the primary direction (axial diffusivity;  $\lambda_1$ ) is more sensitive to the effects of axonal loss or degradation than to demyelination, whereas diffusivity perpendicular to the primary direction (radial diffusivity; the mean of

<sup>1</sup>Duke University Medical Center, <sup>2</sup>Duke University

$\lambda_2$  and  $\lambda_3$ ) is differentially sensitive to demyelination-related effects (Sun et al., 2006; Song et al., 2002, 2003).

Researchers are actively applying DTI to investigating age-related changes in white matter microstructure (Sullivan & Pfefferbaum, 2006; Salat, Tuch, Greve, et al., 2005; Moseley, 2002). The DTI results complement those of the volumetric studies and consistently indicate an age-related decline in FA during adulthood, suggesting a decline in white matter integrity. Sullivan et al. (2001) first reported that age-related decline in FA is relatively more pronounced in prefrontal regions, and this pattern has been confirmed in later studies (Madden et al., 2007; Sullivan, Adalsteinsson, & Pfefferbaum, 2006; Salat, Tuch, Hevelone, et al., 2005; Head et al., 2004). There is regional variability in the degree of age-related decline in FA within the frontal lobe, however, and decline is also notable in the posterior limb of the internal capsule and in the posterior periventricular white matter (Salat, Tuch, Greve, et al., 2005). Analyses of the individual eigenvalues of the diffusion tensor suggest that the age-related decline in prefrontal FA is due almost entirely to increased radial diffusivity, that is, in  $\lambda_2$  and  $\lambda_3$  (Sullivan et al., 2006; Bhagat & Beaulieu, 2004), implicating histopathological mechanisms that pertain to age-related changes in the structure or myelin, rather than a frank loss of axons.

The goal of this research was to determine whether white matter integrity, within specific fiber tracts, mediates age-related changes in cognitive performance. Age-related decline in white matter integrity may contribute to older adults' cognitive performance by disrupting the white matter pathways connecting widely distributed cortical networks (Makris et al., 2007; Pfefferbaum, Adalsteinsson, & Sullivan, 2005; Bartzokis et al., 2004). O'Sullivan et al. (2001) and Sullivan et al. (2001) reported significant correlations between DTI measures of white matter integrity and cognitive performance. Subsequent studies (Bucur et al., 2008; Grieve, Williams, Paul, Clark, & Gordon, 2007; Schulte, Sullivan, Muller-Oehring, Adalsteinsson, & Pfefferbaum, 2005; Madden et al., 2004) have confirmed this pattern, which is most often expressed as a positive relation between performance and FA; that is, individuals with higher levels of white matter integrity exhibit higher levels of task performance.

To conclude that white matter integrity is a mediator of the relation between age and cognitive performance, it is not sufficient to merely demonstrate that a correlation between white matter integrity and a cognitive measure exists, or even that the correlation differs as a function of age group. To establish that variation in white matter integrity operates as a mediating, causal mechanism between age and cognition, rather than as a moderator variable with an associative but not necessarily causal relation, three conditions are necessary (Baron & Kenny, 1986). First, age differences should exist in the measure of cognitive performance; second, age differ-

ences should exist in the measure of white matter integrity; and third, white matter integrity should account for significant variance in cognitive performance, when age is also included in the regression model. These conditions can be tested statistically within the general linear model. A mediating relation exists when the variance in cognitive performance attributable specifically to age is less in the third condition than in the first.

When the amount of age-related variance in a dependent variable (e.g., cognition) is substantially attenuated by the presence of an additional independent variable (e.g., white matter integrity), relative to when age is the sole independent variable, then the additional variable can be interpreted as a mediator of the relation between age and the dependent variable (Salthouse, Atkinson, & Berish, 2003; Salthouse, 1992a). Using this type of analytic approach with  $T_1$ -weighted MRI, Brickman et al. (2006) demonstrated that white matter volume in regions of the frontal lobe mediated adult age differences in neuropsychological tests of executive functioning and memory. To our knowledge, the only DTI study demonstrating a mediational effect of white matter integrity is that of Bucur et al. (2008), who found that the average FA within two regions of interest, the genu of the corpus callosum and a pericallosal frontal region, mediated the relation between elementary perceptual speed and memory retrieval, for younger and older adults combined. The Bucur et al. study, however, did not assess the mediation of *age-related* variance in the behavioral measures.

In the present analyses, we sought to determine whether white matter integrity mediated age-related performance differences in a task-switching paradigm. On each trial, a cue indicated which of two categorization decisions should be performed on an upcoming target word. Performance in this type of task is typically slower and less accurate when the categorization on the current trial switches from the previous trial, relative to when it repeats, reflecting many factors involved in reconfiguring the task set (Monsell, 2003; Meiran, Chorev, & Sapir, 2000). The effects of task switching are more pronounced for older adults than for younger adults (Verhaeghen & Cerella, 2002; Meiran, Gotler, & Perlman, 2001), although the age effects are greater at the global level (i.e., a mixed-task trial block relative to a single-task trial block) than at the local level (i.e., switch trials versus repeat trials). Neuroimaging studies of younger adults suggest that task switching relies on a frontoparietal network that is activated during attention-demanding visual tasks (Braver, Reynolds, & Donaldson, 2003; Kimberg, Aguirre, & D'Esposito, 2000; Sohn, Ursu, Anderson, Stenger, & Carter, 2000).

Analyses of age differences in behavioral measures can be complicated by the overall increase in older adults' reaction time (RT), as well as by individual differences in the relative emphasis on speed versus accuracy. To address this issue, and to isolate different components

of cognitive performance, analyses of the behavioral data were based on the Ratcliff model of two-choice discrimination (Wagenmakers, van der Maas, & Grasman, 2007; Ratcliff, Spieler, & McKoon, 2000; Ratcliff, 1978). This model uses the RT distributions of both correct and incorrect responses to separate the decisional and non-decisional components of performance. The model yields several parameters, the most relevant of which, for the present purposes, are drift rate ( $v$ ; the rate of accumulation toward a decision) and nondecision time ( $T-er$ ; perceptual-motor response time). Thus, we examined the potential role of white matter integrity in these separate aspects of cognitive performance. In our word categorization task, for example, drift rate would reflect the retrieval of semantic information associated with the categorization response, independent of perceptual-motor speed.

We used DTI tractography (Gerig, Gouttard, & Corouge, 2004; Catani, Howard, Pajevic, & Jones, 2002; Mori & van Zijl, 2002) to characterize the diffusion properties of white matter pathways within the fronto-parietal network. We performed tractography analyses for each participant (i.e., in untransformed, native space) to reduce the effect of individual differences in anatomy on tract estimation. The selected pathways were the genu and splenium of the corpus callosum and the superior longitudinal fasciculus (SLF). The genu and the splenium serve as interhemispheric connection pathways for the prefrontal cortex and the occipito-parietal association cortex, respectively, whereas the SLF is a set of pathways connecting the frontal and parietal lobes within each hemisphere (Schmahmann & Pandya, 2006; Makris et al., 2005). Previous DTI studies have reported correlations between FA in these pathways and performance speed (Bucur et al., 2008; Schulte et al., 2005; Madden et al., 2004; Sullivan et al., 2001), but the role of FA as a mediator of *age-related* variance in performance not been examined. In view of the central role of the fronto-parietal network in task switching (Braver et al., 2003; Kimberg et al., 2000; Sohn et al., 2000), we hypothesized that FA in this network would be a mediator of age-related change in task performance. In addition, if white matter integrity within these fronto-parietal regions influences the functioning of task-relevant attentional networks, then FA should mediate age-related changes in the quality of decisional information (drift rate parameter;  $v$ ) rather than perceptual-motor speed (nondecision time parameter;  $T-er$ ).

## METHODS

### Participants

The research procedures were approved by the Institutional Review Board of the Duke University Medical Center, and all participants provided written informed consent. The participants were 20 younger adults (18–

27 years of age; 10 women) and 20 older adults (60–85 years of age; 10 women). The younger adults were recruited from the Duke University campus, and the older adults were healthy, community-dwelling individuals recruited from the Duke Aging Center Research Participant Registry. All participants reported that they were right-handed, free of significant disease such as atherosclerosis and hypertension, and not taking medication known to affect cognitive functioning or cerebral blood flow. Review of each participant's T<sub>2</sub>-weighted structural images by a neuroradiologist (one of the authors, J. M. P.) indicated that all were within normal limits with regard to abnormalities related to atrophy, ventricular dilation, and the presence of white matter hyperintensities.

Demographic and psychometric data (Table 1) were obtained approximately 2 weeks prior to the scanning session. All participants possessed corrected visual acuity of at least 20/40 and possessed at least a secondary school education (12 years). Participants scored a minimum of 27 on the Mini-Mental State Exam (Folstein, Folstein, & McHugh, 1975) and a maximum of 9 on the Beck Depression Inventory (Beck, 1978). During the psychometric testing session, participants also completed a practice version of the task-switching test (with different stimuli) that was used in the subsequent scanning session.

### Behavioral Task

The behavioral task that participants performed during scanning was a version of task switching, modeled after that of Braver et al. (2003). Participants completed six blocks of 51 test trials, corresponding to six fMRI runs.

**Table 1.** Participant Variables by Age Group

	<i>M</i>		<i>SD</i>	
	<i>Younger</i>	<i>Older</i>	<i>Younger</i>	<i>Older</i>
Age (years)	22.40 <sub>a</sub>	69.60 <sub>b</sub>	2.50	6.05
Education (years)	15.75 <sub>a</sub>	16.40 <sub>a</sub>	2.22	2.82
MMSE	29.32 <sub>a</sub>	28.47 <sub>b</sub>	0.60	1.12
BDI	2.65 <sub>a</sub>	2.90 <sub>a</sub>	2.74	2.77
Vocabulary	65.60 <sub>a</sub>	65.05 <sub>a</sub>	3.15	3.80
Digit Symbol Acc	98.52 <sub>a</sub>	95.62 <sub>b</sub>	1.46	1.89
Digit Symbol RT	1338.40 <sub>a</sub>	1836.20 <sub>b</sub>	249.75	314.16

*n* = 20 per age group. Vocabulary = raw score (maximum of 70) on the Wechsler Adult Intelligence Scale—Revised (Wechsler, 1981); BDI = points above zero on the Beck Depression Inventory (Beck, 1978); Digit Symbol Acc and Digit Symbol RT = percentage correct and reaction time (msec), respectively, on a computer test of digit-symbol coding (Salhouse, 1992b); MMSE = raw score (maximum 30) on the Mini-Mental State Exam (Folstein et al., 1975). Means in the same row that do not share subscripts differ by *t* test at *p* < .05.

The fMRI data will be reported in a separate article. Participants viewed the task events with MRI-compatible goggles and responded manually (with the index finger of each hand) via a fiber-optic response box. Within each run, there were three on-task periods, separated by four off-task periods (one of which always occurred at the beginning of the scanner run). This is a mixed blocked/event-related design (Visscher et al., 2003). Each run was approximately 7 min 40 sec in duration, composed of the four off-task periods (19.5 sec each) and three on-task periods (approximately 2 min 7 sec each).

As illustrated in Figure 1, two types of trials occurred during each on-task period: cue-plus-target (12 per on-task period) and cue-only (4 per on-task period). On cue-plus-target trials, participants viewed a cue message and then made a two-choice categorization response to a subsequent target word (a concrete noun). The cue, which was either MAN/NAT or LRG/SML, indicated the type of category decision to be made regarding the target word on the current trial, either manmade/natural or large/small. Manmade/natural referred to artificial (e.g., sailboat) and natural (e.g., lemon) object categories, and large/small referred to whether the referent of the word was larger (e.g., deer) or smaller (e.g., bullet) than a computer monitor. Words were selected to be familiar concrete nouns that could be easily categorized in terms of these criteria. On cue-only trials, the cue message was not followed by a target. These latter trials were included to allow estimation of cue-specific hemodynamic activity and are not reported in the results.

Each cue-plus-target trial was coded as either a repeat or a switch trial, on the basis of whether the associated cue was the same as, or different from, the cue on the immediately preceding trial (even if the preceding trial was cue-only). Within each of the six runs, there were 36 cue-plus-target trials, comprising 18 switch trials and 18 repeat trials. The number of successive trials with the same cue was limited to five. Across the six runs, the two types of categorization decisions, and the two alternative responses within each category, occurred an approximately equal number of times, on both switch and repeat trials.

At the beginning of each run, during the first off-task period, a row of three white fixation crosses appeared in the center of the viewing area for 19.5 sec. These three crosses also remained in view during the other three off-task periods. During the on-task periods (Figure 1), each trial began with a 0.50-sec cue and was followed by a 1.0-sec single fixation cross; the target word then occurred for 1.50 sec. Following the offset of the target, a variable blank period (with a single fixation cross) occurred for either 1.50, 3.0, 4.50, 6.0, or 7.50 sec. The words were presented in large (56 point) white Arial font against a black background. During target word presentation, the two response options were presented at the bottom of the viewing area, at the left and right sides, corresponding to the location of the assigned buttons on the response box. The fixation cross was red following the cue but white following the target, to provide a clear indication of cue-only trials (i.e., the fixation cross changed from red to white). An off-task period followed each (randomized) set of 12 cue-plus-target trials and 4 cue-only trials.

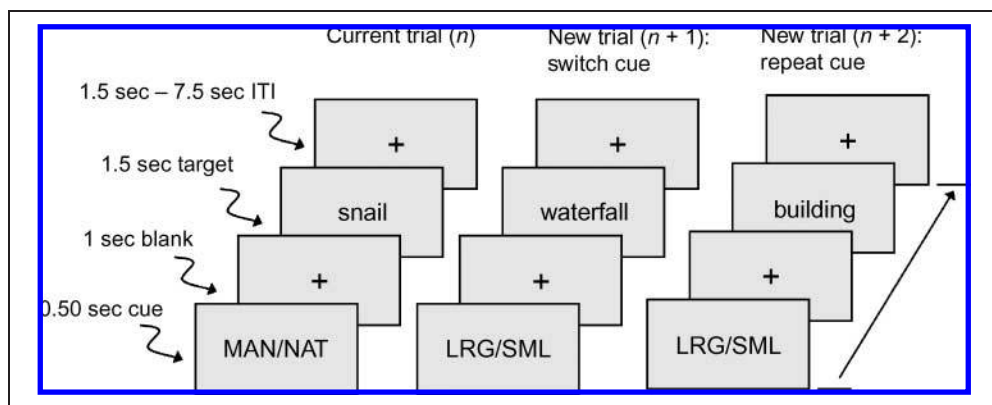
Participants completed one block of 51 practice trials, while situated in the scanner, before performing the test trials. The instructions were to read the cue and to respond as quickly as possible to the target while still being correct. The *manmade* and *large* responses were always assigned to one response button and the *natural* and *small* responses were always assigned to the other button, but the assignment of the response-pairs to the individual buttons was varied across participants within each age group, as was the presentation order of the six blocks of test trials.

## Imaging Protocol

### Acquisition Parameters

Scanning was conducted on a 3-T GE Signa Excite MRI scanner (GE Healthcare, Waukesha, WI) with 50 mT/m gradients, in concert with an eight-channel head coil. Head motion was minimized with a vacuum-pack system molded to each participant's head. Participants wore foam-insert earplugs to counteract scanner noise. The

**Figure 1.** Sequence of events on each trial. The cue display indicated the type of category decision (manmade/natural or larger/smaller than the computer monitor) to be made regarding the target word. Participants responded at the onset of target. Trials are defined as repeat or switch in relation to the cue on the immediately preceding trial. ITI = intertrial interval.



scanning session began with a  $T_1$ -weighted sagittal localizer series, spanning the midline, followed by four other series, in the following order:  $T_1$ -weighted,  $T_2$ -weighted, six runs of  $T_2^*$ -weighted (functional), and two runs of DTI. With the exception of the  $T_1$ -weighted localizer series, slice orientation was near-axial, parallel to the anterior commissure–posterior commissure (AC–PC) plane.

The near-axial  $T_1$ -weighted images were acquired with a high-resolution, 3-D fast inverse-recovery-prepared spoiled gradient recalled (SPGR) sequence ( $256 \times 256$  matrix; TR = 7.4 msec; TE = 3 msec; flip angle =  $12^\circ$ ; FOV = 25.6 cm), yielding 104 contiguous slices of 1.2 mm ( $1 \text{ mm}^2$  in-plane resolution). Each of the DTI sequences used a dual spin echo base sequence ( $128 \times 128$  matrix; TR = 17000 msec; TE = 86.7 msec; flip angle =  $90^\circ$ ; FOV = 25.6 cm), yielding 52 contiguous slices of 2.4 mm ( $1 \text{ mm}^2$  in-plane resolution). Diffusion was measured from 15 non-collinear directions at a  $b$  factor of  $1000 \text{ sec/mm}^2$ ; one reference image had no diffusion weighting. To improve the signal-to-noise ratio, the two DTI runs were merged to a single dataset for each participant. The resulting images were skull-stripped in order to remove nonbrain and ambient noise. We calculated diffusion tensors from the 15 diffusion weighted images, based on a least squares fit of the tensor model to the diffusion data (Basser & Jones, 2002). Diagonalization of the tensor yielded three voxel-specific eigenvalues ( $\lambda_1 > \lambda_2 > \lambda_3$ ), which represent diffusivities along the three principal directions of the tensor.

### Fiber Tracking

The derivation of white matter fiber tracts from the initial DTI datasets was conducted at the individual participant level, in untransformed (native) space, with FiberTracking 2.2.1 and FiberViewer 1.2.3 software ([www.ia.unc.edu/dev/](http://www.ia.unc.edu/dev/); Gerig et al., 2004). The software employs a backtracking method (Mori & van Zijl, 2002) that estimates the direction of greatest diffusivity ( $\lambda_1$ ) between operator-defined *target* and *source* regions, while eliminating fibers terminating in operator-defined *exclusion* regions. Because the 2.4-mm slice thickness of the DTI images was a multiple of the 1.2-mm slice thickness of the  $T_1$ -weighted SPGR images, the latter were resampled to align with the tensors. Four trained operators, blind to participant age, used ITK-SNAP software ([www.itksnap.org/](http://www.itksnap.org/); Yushkevich et al., 2006) to draw target, source, and exclusion regions on the axial slices of each participant's SPGR image. In the case of significant head movement between SPGR and DTI sequence, regions were drawn on the tensor  $b_0$  image. The fiber tracking output comprises representations of fiber bundles that are estimated to pass through the target regions from the source regions, eliminating fibers from the exclusion regions.

We performed tractography for four pathways: fibers coursing through the genu of the corpus callosum,

fibers coursing through the splenium of the corpus callosum connecting to the occipital lobe, fibers of the splenium connecting to the parietal lobe, and fibers associated with the SLF. The target regions in the genu and the splenium were drawn to generate fiber tracts from bilateral sources, and the target regions in the SLF were drawn in the left and right hemispheres separately. Fiber tracking parameters for the genu and the splenium included a minimum FA of 0.15, a fiber tracking threshold (neighborhood voxel coherence) of 0.125, a minimum fiber number of 50, and an angle of maximum deviation of  $35^\circ$ . Because the SLF is more difficult to distinguish from neighboring gray matter than is the corpus callosum, the minimum FA was set to 0.35 for the SLF. Occasional extraneous fibers were eliminated through length-based fiber set thresholding and Hausdorff (distance-based fiber set clustering) methods incorporated into the FiberViewer software.

Examples of target regions, source regions, exclusion regions, and fiber tracts for a single participant are presented in Figure 2. The target regions were defined

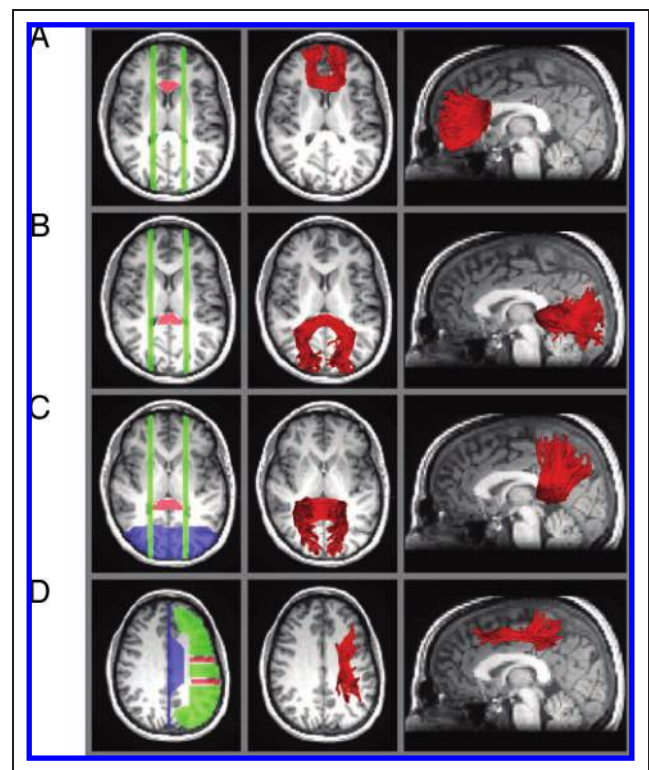


**Figure 2.** Examples of fiber tracts (in red), generated by target and source region placement, for a single participant. The orange areas are target regions, the green areas are source regions, and the blue areas are exclusion regions. All of these regions are operator defined, for each participant, using anatomical boundaries. The fiber tracking algorithm estimates tracts that pass through the target regions from the source regions, eliminating any fibers terminating in the exclusion regions. The approximate locations of output fiber tracts are illustrated by overlaying on a single-slice  $T_1$ -weighted image. (A) genu; (B) splenium–occipital; (C) splenium–parietal; (D) superior longitudinal fasciculus.

using anatomical landmarks (Schmahmann & Pandya, 2006; Makris et al., 2005; Duvernoy, 1999). For the genu and the splenium, we used a method similar to that of Sullivan et al. (2006). We located the target region for the genu using the anterior horns of the lateral ventricle as lateral boundaries (in the axial view), with the anterior cingulate gyrus as the anterior boundary. Operators drew this target region on three to five axial slices, using the presence of the body of the corpus callosum in the axial view as a superior boundary. Source regions for the genu were two parasagittal planes (one per hemisphere; each three slices wide), placed at a point four to six sagittal slices from the axial midline (at approximately the lateral boundaries of the target region), spanning the entire brain in the sagittal view.

The target for the splenium–occipital region was also located on three to five axial slices using the presence of the body of the corpus callosum in the axial view as a superior boundary, although these slices were not constrained to correspond exactly to those used for the genu. In the axial view, the splenium–occipital target region was defined to be a section that is just medial to the posterior horns of the lateral ventricle. The posterior boundary was the posterior cingulate gyrus. Source regions were two parasagittal planes, located similarly to those for the genu, but slightly more lateral, six to eight sagittal slices from the axial midline. To isolate fibers connecting the splenium and the occipital lobe, tract estimation was constrained to exclude any fibers terminating in the parietal lobe.

The splenium–parietal target and source regions were defined similarly to the splenium–occipital case, except that tract estimation was constrained to exclude any fibers terminating in the occipital lobe. As a result of these constraints implemented in the fiber tracking algorithm, the fibers estimated for the splenium–occipital and splenium–parietal regions, although passing through the splenium in each case, were mutually exclusive.

The SLF comprises four anatomical subcomponents (Schmahmann & Pandya, 2006; Makris et al., 2005). We attempted to limit analysis, as much as possible, to SLF II, which occupies the central core of white matter, above the insula, between the frontal and parietal lobes of each hemisphere. Each SLF target region (per hemisphere) spanned three consecutive coronal slices. To define the first, posterior target region, the central sulcus was located in the upper axial slices, and three consecutive coronal slices were selected for the target, with the middle slice positioned at the most lateral point of the central sulcus. The target region on these three coronal slices included gray and white matter from the top of the brain to the lateral fissure, excluding the cingulate gyrus. The second, anterior target region, was also located in the axial view, at the slice just superior to the ventricles. This region comprised three coronal slices, with the middle one positioned at the most lateral point of the precentral sulcus. This region

also included the gray and white matter between the top of the brain and the lateral fissure, excluding the cingulate gyrus.

Operators drew three source regions for the SLF; these spanned the axial slices between the top of the brain and the top of the ventricles, excluding the cingulate gyrus, within each hemisphere. The first source comprised frontal lobe gray and white matter anterior to the anterior target region, the second source was the gray and white matter between the anterior and posterior target regions; and the third source was gray and white matter between the posterior target region and the parieto-occipital sulcus. Tract estimation was additionally constrained to exclude fibers terminating in the temporal or occipital lobe.

Within the genu and splenium regions, tract length was limited to 18 mm on either side of the axial midline. We divided the genu and the splenium into center, left, and right segments, using a point 5 mm on either side of the midline 0 value as the lateral boundaries of the center segment, and 6 to 18 mm on either side as the left and right segments. For the SLF, tract length was limited to 18 mm anterior and posterior to the central sulcus (i.e., anterior and posterior segments of 18 mm each).

## RESULTS

### Task-switching Performance

#### *Mean Reaction Time and Error Rate*

We eliminated those cue-plus-target trials on which the participant either did not respond or responded with an RT <300 msec or >2500 msec (<2% of trials within each age group). The mean RT for correct responses (across all six runs) and the mean percentage accuracy are presented in Table 2. ANOVA of the mean RT data, using age group as a between-subjects variable and task condition (switch, repeat) as a within-subjects variable, yielded only a main effect of age group [ $F(1, 38) = 15.56, p < .001$ ], reflecting the age-related increase in

**Table 2.** Mean Reaction Time and Error Rate, in Task Switching, by Age Group and Task Condition

	<i>M</i>		<i>SD</i>	
	<i>Younger</i>	<i>Older</i>	<i>Younger</i>	<i>Older</i>
<i>Repeat Trials</i>				
Reaction time (msec)	897.30	1038.12	105.34	124.97
Accuracy (%)	95.46	93.47	2.22	3.71
<i>Switch Trials</i>				
Reaction time (msec)	899.06	1046.09	115.40	118.04
Accuracy (%)	92.27	91.44	2.92	2.68

*n* = 20 per age group.

RT. For accuracy, only the main effect of condition was significant [ $F(1, 38) = 44.90, p < .0001$ ], reflecting the higher accuracy for repeat trials than for switch trials.

### Reaction Time Model

We separated the decisional and nondecisional components of performance with a simplified version of the Ratcliff model of two-choice discrimination (Ratcliff et al., 2000; Ratcliff, 1978) developed by Wagenmakers et al. (2007). The Wagenmakers et al. implementation combines the information from the mean and variance of RT for correct responses, and the mean accuracy, for each participant, to estimate three parameters: the quality of decision information (drift rate;  $\nu$ ), the time required for perceptual-motor processes (nondecision time;  $T_{-er}$ ), and response conservativeness (cautiousness;  $a$ ). We obtained separate estimates of drift rate and nondecision time for the repeat and switch trials. The drift rate, representing the accumulation of information, can vary as a function of the decision process on each trial. Although nondecision time should not, in theory, vary across different types of trials intermixed within a block, we analyzed nondecision time for switch and repeat trials separately because there is evidence that task difficulty can influence the nondecision time parameter (Spaniol, Madden, & Voss, 2006). Analysis of the cautiousness parameter was limited to the participant level because the participants' response conservativeness (i.e., amount of evidence required for a particular response) should not fluctuate systematically within a block of trials.

ANOVA of the drift rate and nondecision time data (Figure 3) treated age group as a between-subjects variable and task condition (repeat vs. switch) as a within-subjects variable. Significant main effects of age group indicated that older adults exhibited a lower drift rate [ $F(1, 38) = 10.74, p < .01$ ] and a higher nondecision time [ $F(1, 38) = 6.84, p < .05$ ] than younger adults. Switch trials were associated with a lower drift rate [ $F(1, 38) = 36.52, p < .0001$ ] and a higher nondecision time [ $F(1, 38) = 5.80, p < .05$ ] than repeat trials. The Age

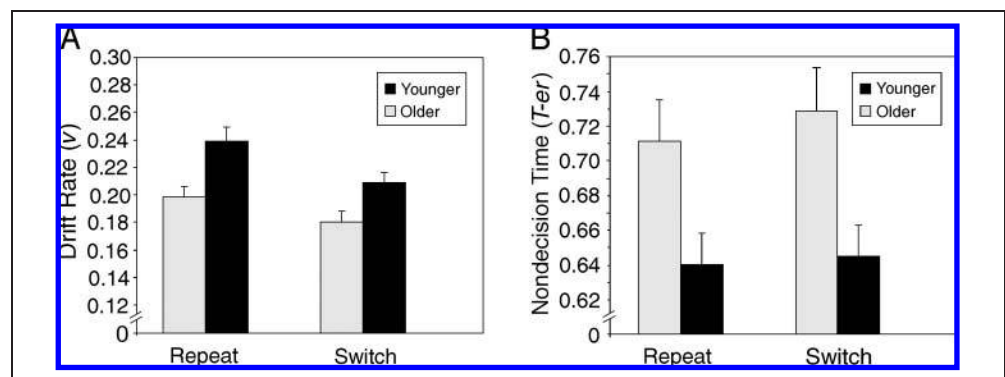
group  $\times$  Task condition interaction was not significant for either drift rate or nondecision time. The value of the  $a$  parameter was higher for older adults ( $M = 0.14$ ;  $SD = 0.02$ ) than for younger adults ( $M = 0.13$ ;  $SD = 0.02$ ) [ $t(38) = 2.65, SE = 0.005, p < .01$ ], indicating an age-related increase in cautiousness.

### Fiber Tracking Data

Mean FA values within the estimated fiber tracts, at millimeter intervals along the estimated tract, are presented in Figure 4. (Splenium-parietal data for one older adult were eliminated because the fiber tracking algorithm did not generate the minimum number of 50 fibers.) We performed ANOVAs of FA for each region, using age group as a between-subjects variable, and segment as a within-subjects variable. For the SLF, hemisphere was an additional within-subjects variable. The results of these analyses (Table 3) confirm the pattern evident in Figure 4: For each of the four regions, there was a significant main effect of age group, reflecting an age-related decline in FA. Each region also exhibited a significant effect of segment. In the case of the genu and both splenium regions, this effect represented a decline in FA for the peripheral segments relative to the central segment. For the SLF, the segment effect represented lower FA values anterior to the central sulcus than posterior to it.

In the FA analyses of the regions, two Age group  $\times$  Segment interactions were significant, indicating variation in the age difference as a function of the segment within the region. The first Age group  $\times$  Segment interaction, for the genu, resulted from a more pronounced age-related decline in FA for the peripheral segments than for the central segment. (The splenium-parietal data exhibited a marginally significant trend toward a similar pattern.) The second Age group  $\times$  Segment effect, for the SLF, occurred as the result of greater age-related decline in FA anterior to the central sulcus than in the more posterior segment of this tract. The SLF also exhibited a Hemisphere  $\times$  Segment interaction

**Figure 3.** Mean parameter estimates (Wagenmakers et al., 2007) of task-switching performance, as a function of age group and repeat versus switch trials. (A) The drift rate parameter ( $\nu$ ), representing the quality of decision processing; (B) The nondecision time parameter ( $T_{-er}$ ), representing perceptual encoding and response time.



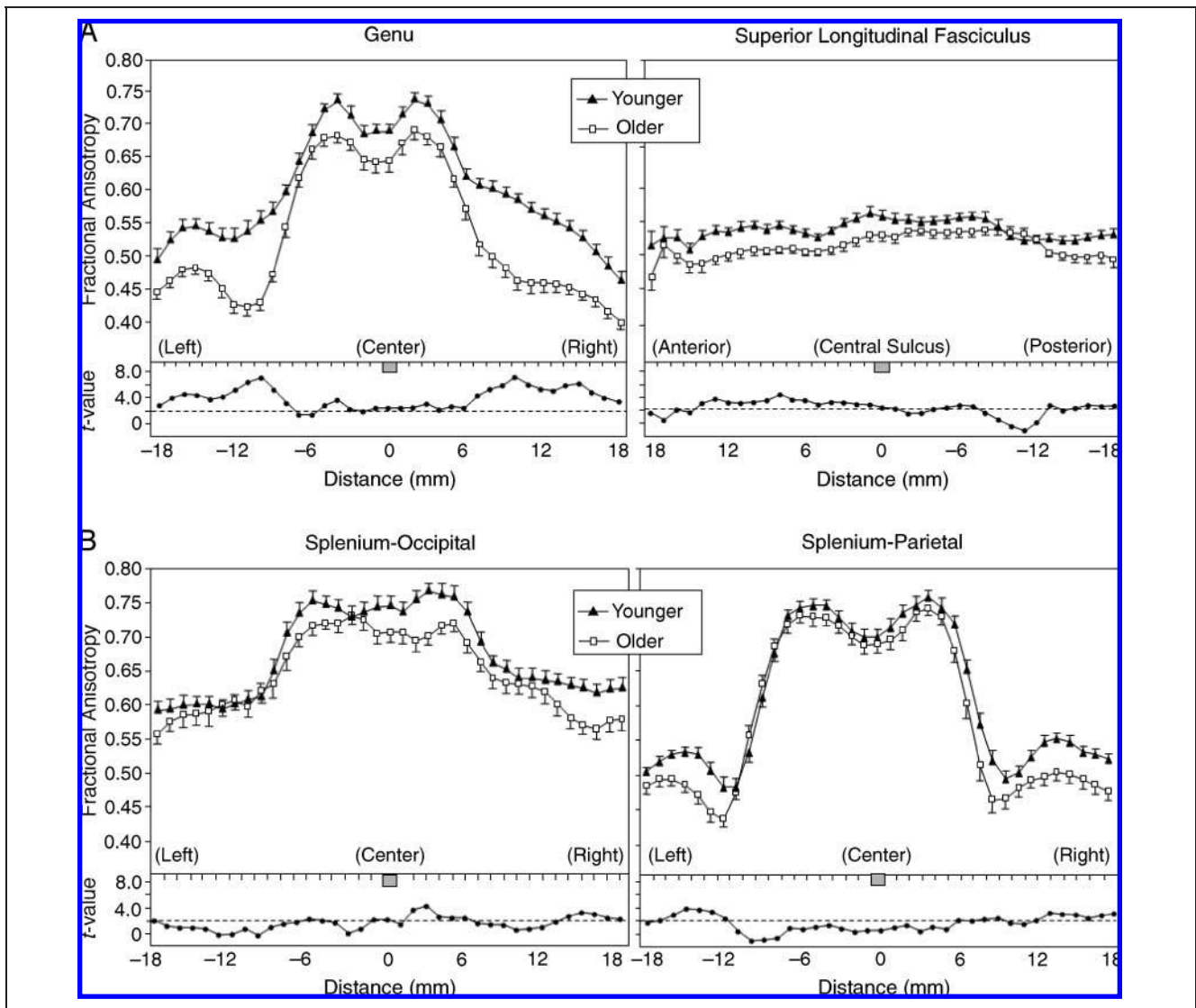


**Figure 4.** Mean fractional anisotropy (FA) as a function of age group and interval along the tract. Error bars represent 1 SE. (A) Genu and superior longitudinal fasciculus; (B) Splenium–occipital and splenium–parietal. For the genu and the splenium, the tracts are oriented left–right, with 0 = axial midline. For the SLF, the tracts are oriented anterior–posterior and 0 = central sulcus. Below the mean FA data,  $t$  values are plotted for the age group comparison at each point along the tract. The dotted line represents the significant  $t(38)$  value for  $p < .05$ , two-tailed.

because the lower mean FA for the anterior segment, relative to the posterior segment, was present for both hemispheres but was greater for the left hemisphere ( $M$  difference in FA of 0.0179) than for the right hemisphere ( $M$  difference in FA of 0.0026).

We also conducted analyses of the age difference for axial diffusivity ( $\lambda_1$ ) and radial diffusivity (mean of  $\lambda_2$  and  $\lambda_3$ ) separately (averaged over within-tract segments), to test previous observations that age-related change is specific to radial diffusivity (Sullivan et al., 2006; Bhagat & Beaulieu, 2004). The most important aspect of these results, illustrated in Figure 5, is that no region exhibited a significant age difference in axial diffusivity. Significant age-related increases in radial diffusivity occurred for the genu [ $F(1, 38) = 19.15, p < .0001$ ] and the SLF [ $F(1, 38) = 8.62, p < .01$ ], with a similar,

although marginal, effect in the splenium–occipital region [ $F(1, 38) = 3.76, p < .06$ ].

### Mediation of Task Switching by White Matter Integrity

We limited the mediation analyses to the performance measures of drift rate and nondecision time because these latter measures (unlike the cautiousness parameter) reflect the quality of information processing for individual decisions, which in turn would rely on the integrity of task-relevant neural networks. In addition, because our goal was to determine the mediation of age-related effects, and the magnitude of the age group differences in drift rate and nondecision time did not vary significantly as a function of switch versus repeat

**Table 3.** Significant ANOVA Effects for Fractional Anisotropy

Region	Effect	df	F	p
Genu	Grp	1, 38	40.03	<.0001
	Segment	2, 76	578.58	<.0001
	Grp × Segment	2, 76	7.39	.0012
SLF	Grp	1, 38	22.18	<.0001
	Segment	1, 38	13.34	.0008
	Grp × Segment	1, 38	6.43	.0155
	Hem × Segment	1, 38	5.65	.0226
Splenium–occipital	Grp	1, 38	8.93	.0049
	Segment	2, 76	172.52	<.0001
Splenium–parietal	Grp	1, 37	8.31	.0065
	Segment	2, 74	480.09	<.0001
	Grp × Segment	2, 74	2.77	.0693

SLF = superior longitudinal fasciculus; Grp = age group; Hem = hemisphere; Segment = center, left, right for genu and splenium regions; Segment = anterior, posterior for SLF;  $n = 20$  per age group except for older adults' splenium–parietal, where  $n = 19$ .

trials, we averaged over these different trial types and obtained a single drift rate and nondecision time for each participant.

For both nondecision time and drift rate, regression models were developed for each regional FA value as a predictor of performance, with age group included in the model (i.e., covaried). Three fiber-tract segments (splenium–occipital left, splenium–parietal center, and SLF left posterior) were excluded from further analyses because they did not exhibit a significant age-related change (Table 4). For nondecision time, none of the 10 candidate FA values was significant as a predictor when covaried for age group. For drift rate, age-covaried FA values from two regions were significant as predictors: genu

center,  $\beta = 0.249$ ,  $SE = 0.124$ ,  $p = .05$ ; and splenium–parietal right,  $\beta = 0.348$ ,  $SE = 0.151$ ,  $p < .05$ . Parameter estimates for both regions were positive, indicating that individuals with higher FA values also had higher drift rates (i.e., increased white matter integrity was associated with more efficient accumulation of evidence).

We used hierarchical regression to estimate the amount of age-related variance in drift rate, when FA was entered into the model before age group, relative to when age group was the only predictor (Salthouse, 1992a). The unique variance in drift rate associated with age group, following FA, divided by the variance associated with age group as the sole predictor, is an indicator of the degree to which FA attenuates the age-related variance.

The results, illustrated in Figure 6, indicate that when used as sole predictors, there were significant components of variance in drift rate for age group ( $\beta = -0.174$ ,  $SE = 0.005$ ,  $p < .01$ ), genu center ( $\beta = 0.367$ ,  $SE = 0.116$ ,  $p < .01$ ), and splenium–parietal right ( $\beta = 0.482$ ,  $SE = 0.130$ ,  $p < .001$ ). When entered before age group, the splenium–parietal right FA variable led to a substantial attenuation in age-related variance, and age group did not remain significant as a predictor of drift rate. The genu center FA variable, when entered before age group, also led to a pronounced attenuation in the age-related variance in drift rate, although age group remained significant as a predictor ( $\beta = -0.123$ ,  $SE = 0.006$ ,  $p < .05$ ).

## DISCUSSION

### DTI Findings

Using DTI tractography, we characterized white matter integrity within several pathways of the fronto-parietal network and tested whether integrity (as indexed by FA) in this network mediated adult age differences in cognitive performance during task switching. We relied

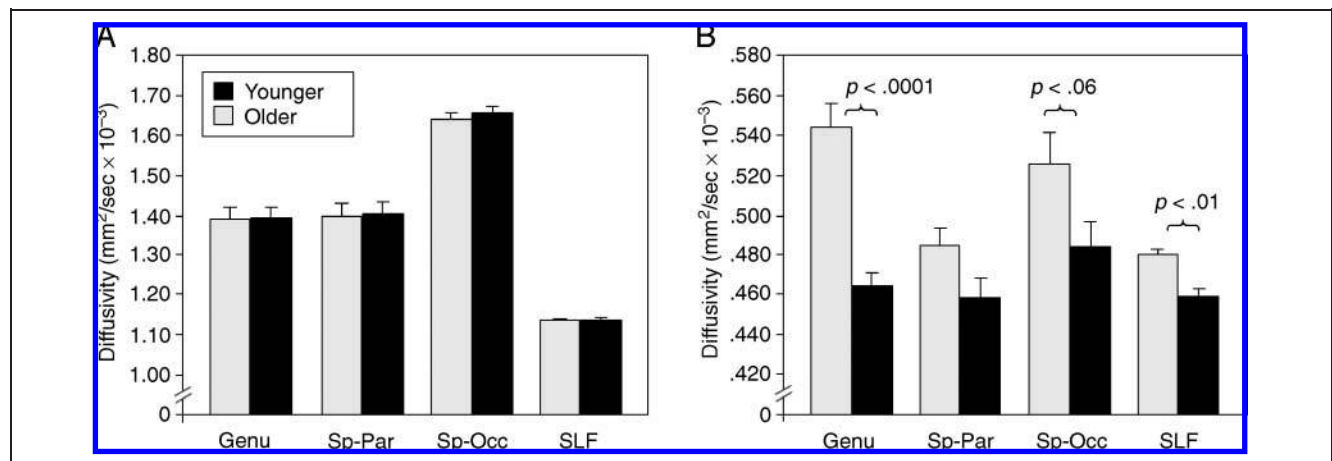


**Figure 5.** Diffusivity as a function of age group and region. (A) Axial diffusivity (the first eigenvalue,  $\lambda_1$ ); (B) radial diffusivity (the mean of the second and third eigenvalues,  $\lambda_2$ , and  $\lambda_3$ ). Sp-Par = splenium–parietal; Sp-Occ = splenium–occipital; SLF = superior longitudinal fasciculus.

**Table 4.** Test of Age Group Difference in Mean Fractional Anisotropy by Region

Region	<i>M</i>		<i>SD</i>		<i>t</i>	<i>df</i>	<i>p</i>
	Younger	Older	Younger	Older			
Genu center	0.7088	0.6628	0.0272	0.0567	3.27	38	.0023
Genu left	0.5624	0.4915	0.0277	0.0414	6.36	38	<.0001
Genu right	0.5570	0.4677	0.0286	0.0489	7.05	38	<.0001
Splenium–occipital center	0.7490	0.7129	0.0454	0.0417	2.62	38	.0125
Splenium–occipital left	0.6357	0.6178	0.0303	0.0398	1.59	38	.1195
Splenium–occipital right	0.6481	0.6129	0.0345	0.0409	2.94	38	.0056
Splenium–parietal center	0.7275	0.7138	0.0482	0.0412	0.95	37	.3466
Splenium–parietal left	0.5674	0.5468	0.0269	0.0311	2.21	37	.0332
Splenium–parietal right	0.5552	0.5119	0.0343	0.0344	3.94	37	.0004
SLF right anterior	0.5449	0.5108	0.0174	0.0248	5.05	38	<.0001
SLF right posterior	0.5420	0.5189	0.0225	0.0192	3.50	38	.0012
SLF left anterior	0.5393	0.5101	0.0356	0.0229	3.08	38	.0038
SLF left posterior	0.5485	0.5368	0.0250	0.0136	1.85	38	.0721

SLF = superior longitudinal fasciculus.  $n = 20$  per age group except for the older adults' splenium–parietal region, where  $n = 19$ .

on the definition of mediation by Baron and Kenny (1986), which required that several conditions be met: the existence of age differences in both cognitive performance and FA, and a significant relation between FA and cognition when age-related effects in cognition were controlled statistically. The main finding was that, as hy-

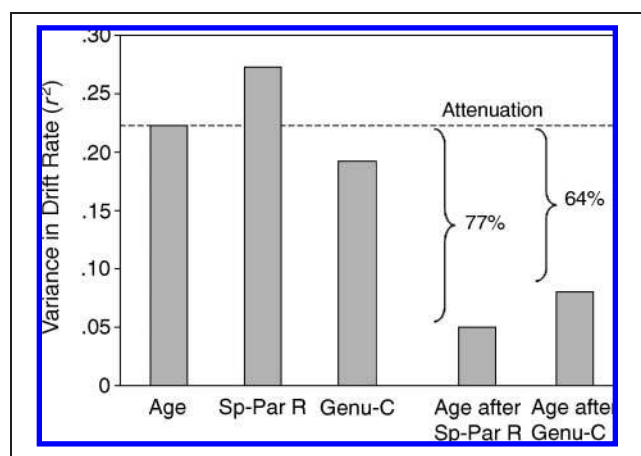


**Figure 6.** Attenuation of age-related variance in drift rate (decisional processing) by regional FA. The first three bars (from left to right) in the graph illustrate the variance in drift rate associated with age group, FA in the right-hemisphere splenium–parietal tract (Sp–Par R), and FA in the central genu (Genu-C), when each of these variables is used as the sole predictor of drift rate. The last two bars in the graph illustrate the attenuation of age-related variance when either the splenium or genu FA variables are entered before age group in the regression model. The substantial attenuation indicates that these variables are mediators of age differences in this aspect of task performance.

pothesized, mean FA in two regions, the central portion of the genu, and the splenium–parietal fibers in the right hemisphere, was related to performance independently of age and provided substantial attenuation of the age-related variance in performance (Figure 6). In addition, as discussed below, FA was related to a measure of the quality of decisional information and not to the perceptual–motor (nondecisional) component. The present study is, to our knowledge, the first demonstration of the mediation of age-related differences in cognitive performance by white matter integrity.

Age-related decline in FA was distributed throughout nearly all of the selected pathways. The decline was numerically greatest the peripheral segments of the genu (Figure 4), consistent with previous observations of greater age-related decline in FA in anterior brain regions (Sullivan & Pfefferbaum, 2006; Sullivan et al., 2001, 2006; Head et al., 2004). The analysis of axial and radial diffusivity suggested that the age-related changes in FA were not equally apparent in all three eigenvalues but were instead limited entirely to radial diffusivity (Figure 5). This age-related increase in diffusivity perpendicular to the primary eigenvalue confirms previous findings (Sullivan et al., 2006; Bhagat & Beaulieu, 2004) and suggests that the primary neurobiological mechanism of age-related change in white matter integrity is decreased integrity of myelin rather than axonal damage or loss (Sun et al., 2006; Song et al., 2002, 2003). However, the contributions of axonal loss (Marnier et al., 2003) to changes in DTI assessments of cerebral white matter in the aging brain are not well understood and may also result in age-related increases in  $\lambda_2$  and  $\lambda_3$ .

The two regions that we found to be mediators, the genu and the splenium of the corpus callosum, have been identified previously in correlational studies of white matter and behavior. Previous studies have found that increased perceptual speed is associated with increased white matter integrity in the genu (Bucur et al., 2008; Schulte et al., 2005; Sullivan et al., 2001). White matter integrity of the splenium has also exhibited similar correlations with speed-dependent measures (Madden et al., 2004; Sullivan et al., 2001). The present data suggest that splenium fibers leading to the parietal lobe, especially in the right hemisphere, are related more closely to age differences in cognitive performance than are splenium–occipital fibers. The cortical network that is active during task switching involves dorsolateral prefrontal and superior parietal regions (Braver et al., 2003; Kimberg et al., 2000; Sohn et al., 2000). Previous fMRI investigations of visual attention have also noted that attention-dependent parietal activations are relatively greater in the right hemisphere (Corbetta & Shulman, 2002; Kim et al., 1999). Age-related decline in white matter integrity would lead to some degree of graded, functional disconnection among task-relevant cortical regions in the fronto-parietal network (Makris et al., 2007; Sullivan & Pfefferbaum, 2006; Pfefferbaum et al., 2005; Bartzokis et al., 2004; O’Sullivan et al., 2001).

Current models of age-related change in brain function frequently propose that age-related deficits in cognitive performance reflect the interactive effects of structural changes in the frontal lobe and the compensatory recruitment of these regions to support task performance (Davis, Dennis, Daselaar, Fleck, & Cabeza, 2008; Dennis & Cabeza, 2008; Cabeza, 2002; Grady, 2000). In view of the mediational effects associated with the splenium as well as the genu, however, we emphasize that white matter integrity of posterior brain regions is also relevant. The cortical networks activated by attention-demanding tasks are distributed widely and vulnerable to disruption at posterior as well as anterior sites (Andrews-Hanna et al., 2007; Tisserand & Jolles, 2003; Greenwood, 2000). In addition, although age-related decline in FA for the SLF was greater in the portion of this pathway anterior to the central sulcus than posterior to it, the anterior SLF was not a significant mediator of age differences in performance. Thus, although age-related decline may be detected more frequently within anterior brain regions, whether a particular white matter region serves as a behavioral mediator is not dependent on the magnitude of age-related decline in FA for that region (Madden et al., 2004).

The tractography method that we used, applied at the individual participant level, has the advantage of taking individual differences in anatomy into account, but several sources of error exist, including the thresholding, the use of nonisotropic voxel dimensions, the presence of crossing fibers, and partial volume effects. It would consequently be valuable to have converging evidence,

regarding the age differences in white matter integrity that we have observed, from tractography based on spatially normalized data and isotropic voxel dimensions.

## Behavioral Findings

We separated the decisional and nondecisional components of performance by applying a quantitative model that combines information from the distribution of RT and accuracy across trials (Wagenmakers et al., 2007; Ratcliff et al., 2000; Ratcliff, 1978). This model has been applied previously to age differences in other forms of two-choice discrimination (Spaniol et al., 2006; Ratcliff, Thapar, & McKoon, 2004), but has not been investigated in the context of task switching. The results (Figure 3) demonstrated that, relative to younger adults, older adults exhibited both a decline in the quality of the decisional component (drift rate,  $v$ ), and an increase in the time required by nondecisional, encoding and response processes ( $T\text{-er}$ ). We also obtained an age-related increase in cautiousness ( $a$ ). These findings confirm previous age-related effects in applications of this model (Spaniol et al., 2006; Ratcliff et al., 2004). New findings were the decreased drift rate and increased nondecision time for switch trials, relative to repeat trials, reflecting the increased attentional demands of task switching as expressed in these model parameters. The effects of aging and task switching were not interactive, however, and the increased difficulty of the switch trials relative to repeat trials was similar for the two age groups. This pattern is consistent with previous studies of age differences in task switching. Global switch costs (i.e., the difference between tasks involving switching and those involving a single, constant decision) are typically higher for older adults than for younger adults, whereas local switch costs (i.e., the cost of switching across adjacent trials) are less age-dependent (Verhaeghen & Cerella, 2002; Meiran et al., 2001).

Because the difference between switch and repeat trials was similar for the two age groups, we averaged across these trials to investigate the mediation of age-related effects in the drift rate and nondecision time measures. The mediational effect of white matter integrity that we observed (Figure 6) consequently refers to performance of the manmade/natural and large/small categorization decisions, independently of the effects of switching between these tasks. The role of white matter integrity, however, was specific to the decisional component of this categorization (e.g., retrieval of the requisite semantic information); mediation was not associated with time required for nondecisional processes. Paus et al. (2001) emphasized that, in studies of white matter–behavioral correlations, information processing tasks have an advantage, relative to standardized psychometric tests, by providing better access to the “building blocks” of cognitive abilities. The present findings support the Paus et al. proposal and suggest that correlations between FA and

behavioral measures (Sullivan & Pfefferbaum, 2006) are not dependent entirely on perceptual–motor processing and may instead reflect decision-level processing. Application of tractography to pathways more directly involved with perceptual–motor processing (e.g., corticospinal tracts) may yield correlations between FA and nondecision time. From the present results, we conclude that some decision-related processes operate less efficiently for older adults than for younger adults, and that age-related decline in the white matter integrity within specific regions of the fronto-parietal network (central genu and splenium–parietal fibers in the right hemisphere) has a causal role in this form of age-related cognitive change.

## Acknowledgments

This research was supported by NIH research grants R01 AG011622 (D. J. M.), R01 AG019731 and R01 AG23770 (R. C.), R21 AG30771 (S. A. H.), and NIH training grant T32 AG000029 (M. C. C., B. B., and N. A. D.). We thank Susanne M. Harris, Anne M. Shepler, and Leslie Crandell Dawes for technical assistance, and Allen Song for advice during this research.

Reprint requests should be sent to David J. Madden, Box 2980, Duke University Medical Center, Durham, NC 27710, or via e-mail: djm@geri.duke.edu, david.madden@duke.edu.

## REFERENCES

- Andrews-Hanna, J. R., Snyder, A. Z., Vincent, J. L., Lustig, C., Head, D., Raichle, M. E., et al. (2007). Disruption of large-scale brain systems in advanced aging. *Neuron*, *56*, 924–935.
- Baron, R. M., & Kenny, D. A. (1986). The moderator–mediator variable distinction in social psychological research: Conceptual, strategic, and statistical considerations. *Journal of Personality and Social Psychology*, *51*, 1173–1182.
- Bartzikis, G., Sultzer, D., Lu, P. H., Nuechterlein, K. H., Mintz, J., & Cummings, J. L. (2004). Heterogeneous age-related breakdown of white matter structural integrity: Implications for cortical “disconnection” in aging and Alzheimer’s disease. *Neurobiology of Aging*, *25*, 843–851.
- Basser, P. J., & Jones, D. K. (2002). Diffusion-tensor MRI: Theory, experimental design and data analysis—A technical review. *NMR in Biomedicine*, *15*, 456–467.
- Beaulieu, C. (2002). The basis of anisotropic water diffusion in the nervous system—A technical review. *NMR in Biomedicine*, *15*, 435–455.
- Beck, A. T. (1978). *The Beck Depression Inventory*. New York: Psychological Corporation.
- Bhagat, Y. A., & Beaulieu, C. (2004). Diffusion anisotropy in subcortical white matter and cortical gray matter: Changes with aging and the role of CSF-suppression. *Journal of Magnetic Resonance Imaging*, *20*, 216–227.
- Braver, T. S., Reynolds, J. R., & Donaldson, D. I. (2003). Neural mechanisms of transient and sustained cognitive control during task switching. *Neuron*, *39*, 713–726.
- Brickman, A. M., Zimmerman, M. E., Paul, R. H., Grieve, S. M., Tate, D. F., Cohen, R. A., et al. (2006). Regional white matter and neuropsychological functioning across the adult lifespan. *Biological Psychiatry*, *60*, 444–453.
- Bucur, B., Madden, D. J., Spaniol, J., Provenzale, J. M., White, L. E., Cabeza, R., et al. (2008). Age-related slowing of memory retrieval: Contributions of perceptual speed and cerebral white matter integrity. *Neurobiology of Aging*, *29*, 1070–1079.
- Cabeza, R. (2002). Hemispheric asymmetry reduction in older adults: The HAROLD model. *Psychology and Aging*, *17*, 85–100.
- Catani, M., Howard, R. J., Pajevic, S., & Jones, D. K. (2002). Virtual in vivo interactive dissection of white matter fasciculi in the human brain. *Neuroimage*, *17*, 77–94.
- Corbetta, M., & Shulman, G. L. (2002). Control of goal-directed and stimulus-driven attention in the brain. *Nature Reviews Neuroscience*, *3*, 201–215.
- Davis, S. W., Dennis, N. A., Daselaar, S. M., Fleck, M. S., & Cabeza, R. (2008). Que PASA? The posterior anterior shift in aging. *Cerebral Cortex*, *18*, 1201–1209.
- Dennis, N. A., & Cabeza, R. (2008). Neuroimaging of healthy cognitive aging. In F. I. M. Craik & T. A. Salthouse (Eds.), *The handbook of aging and cognition* (3rd ed., pp. 1–54). New York: Psychology Press.
- Duvernoy, H. M. (1999). *The human brain: Surface, three-dimensional sectional anatomy with MRI, and blood supply* (2nd ed.). New York: Springer-Verlag.
- Folstein, M. F., Folstein, S. E., & McHugh, P. R. (1975). “Mini-mental state”. A practical method for grading the cognitive state of patients for the clinician. *Journal of Psychiatric Research*, *12*, 189–198.
- Gerig, G., Gouttard, S., & Corouge, I. (2004). Analysis of brain white matter via fiber tract modeling. *Conference Proceedings of the 26th Annual International Conference of the IEEE Engineering in Medicine and Biology Society*, *6*, 4421–4424.
- Grady, C. L. (2000). Functional brain imaging and age-related changes in cognition. *Biological Psychology*, *54*, 259–281.
- Greenwood, P. M. (2000). The frontal aging hypothesis evaluated. *Journal of the International Neuropsychological Society*, *6*, 705–726.
- Grieve, S. M., Williams, L. M., Paul, R. H., Clark, C. R., & Gordon, E. (2007). Cognitive aging, executive function, and fractional anisotropy: A diffusion tensor MR imaging study. *AJNR, American Journal of Neuroradiology*, *28*, 226–235.
- Guttmann, C. R., Jolesz, F. A., Kikinis, R., Killiany, R. J., Moss, M. B., Sandor, T., et al. (1998). White matter changes with normal aging. *Neurology*, *50*, 972–978.
- Head, D., Buckner, R. L., Shimony, J. S., Williams, L. E., Akbudak, E., Conturo, T. E., et al. (2004). Differential vulnerability of anterior white matter in nondemented aging with minimal acceleration in dementia of the Alzheimer type: Evidence from diffusion tensor imaging. *Cerebral Cortex*, *14*, 410–423.
- Kim, Y. H., Gitelman, D. R., Nobre, A. C., Parrish, T. B., LaBar, K. S., & Mesulam, M. M. (1999). The large-scale neural network for spatial attention displays multifunctional overlap but differential asymmetry. *Neuroimage*, *9*, 269–277.
- Kimberg, D. Y., Aguirre, G. K., & D’Esposito, M. (2000). Modulation of task-related neural activity in task-switching: An fMRI study. *Brain Research, Cognitive Brain Research*, *10*, 189–196.
- Le Bihan, D. (2003). Looking into the functional architecture of the brain with diffusion MRI. *Nature Reviews Neuroscience*, *4*, 469–480.
- Madden, D. J., Spaniol, J., Whiting, W. L., Bucur, B., Provenzale, J. M., Cabeza, R., et al. (2007). Adult age differences in the functional neuroanatomy of visual attention: A combined fMRI and DTI study. *Neurobiology of Aging*, *28*, 459–476.

- Madden, D. J., Whiting, W. L., Huettel, S. A., White, L. E., MacFall, J. R., & Provenzale, J. M. (2004). Diffusion tensor imaging of adult age differences in cerebral white matter: Relation to response time. *Neuroimage*, *21*, 1174–1181.
- Makris, N., Kennedy, D. N., McInerney, S., Sorensen, A. G., Wang, R., Caviness, V. S., Jr., et al. (2005). Segmentation of subcomponents within the superior longitudinal fascicle in humans: A quantitative, in vivo, DT-MRI study. *Cerebral Cortex*, *15*, 854–869.
- Makris, N., Papadimitriou, G. M., van der Kouwe, A., Kennedy, D. N., Hodge, S. M., Dale, A., et al. (2007). Frontal connections and cognitive changes in normal aging rhesus monkeys: A DTI study. *Neurobiology of Aging*, *10*, 1556–1567.
- Marnier, L., Nyengaard, J. R., Tang, Y., & Pakkenberg, B. (2003). Marked loss of myelinated nerve fibers in the human brain with age. *Journal of Comparative Neurology*, *462*, 144–152.
- Meiran, N., Chorev, Z., & Sapir, A. (2000). Component processes in task switching. *Cognitive Psychology*, *41*, 211–253.
- Meiran, N., Gotler, A., & Perlman, A. (2001). Old age is associated with a pattern of relatively intact and relatively impaired task-set switching abilities. *Journals of Gerontology: Series B, Psychological Sciences and Social Sciences*, *56*, P88–P102.
- Monsell, S. (2003). Task switching. *Trends in Cognitive Sciences*, *7*, 134–140.
- Mori, S., & van Zijl, P. C. (2002). Fiber tracking: Principles and strategies—A technical review. *NMR in Biomedicine*, *15*, 468–480.
- Moseley, M. (2002). Diffusion tensor imaging and aging—A review. *NMR in Biomedicine*, *15*, 553–560.
- O'Sullivan, M., Jones, D. K., Summers, P. E., Morris, R. G., Williams, S. C., & Markus, H. S. (2001). Evidence for cortical “disconnection” as a mechanism of age-related cognitive decline. *Neurology*, *57*, 632–638.
- Paus, T., Collins, D. L., Evans, A. C., Leonard, G., Pike, B., & Zijdenbos, A. (2001). Maturation of white matter in the human brain: A review of magnetic resonance studies. *Brain Research Bulletin*, *54*, 255–266.
- Pfefferbaum, A., Adalsteinsson, E., & Sullivan, E. V. (2005). Frontal circuitry degradation marks healthy adult aging: Evidence from diffusion tensor imaging. *Neuroimage*, *26*, 891–899.
- Ratcliff, R. (1978). A theory of memory retrieval. *Psychological Review*, *85*, 59–108.
- Ratcliff, R., Spieler, D., & McKoon, G. (2000). Explicitly modeling the effects of aging on response time. *Psychonomic Bulletin & Review*, *7*, 1–25.
- Ratcliff, R., Thapar, A., & McKoon, G. (2004). A diffusion model analysis of the effects of aging on recognition memory. *Journal of Memory and Language*, *50*, 408–424.
- Raz, N. (2005). The aging brain observed in vivo: Differential changes and their modifiers. In R. Cabeza, L. Nyberg, & D. Park (Eds.), *Cognitive neuroscience of aging: Linking cognitive and cerebral aging* (pp. 19–57). Oxford: Oxford University Press.
- Raz, N., Lindenberger, U., Rodrigue, K. M., Kennedy, K. M., Head, D., Williamson, A., et al. (2005). Regional brain changes in aging healthy adults: General trends, individual differences and modifiers. *Cerebral Cortex*, *15*, 1676–1689.
- Resnick, S. M., Pham, D. L., Kraut, M. A., Zonderman, A. B., & Davatzikos, C. (2003). Longitudinal magnetic resonance imaging studies of older adults: A shrinking brain. *Journal of Neuroscience*, *23*, 3295–3301.
- Salat, D. H., Kaye, J. A., & Janowsky, J. S. (1999). Prefrontal gray and white matter volumes in healthy aging and Alzheimer's disease. *Archives of Neurology*, *56*, 338–344.
- Salat, D. H., Tuch, D. S., Greve, D. N., van der Kouwe, A. J., Hevelone, N. D., Zaleta, A. K., et al. (2005). Age-related alterations in white matter microstructure measured by diffusion tensor imaging. *Neurobiology of Aging*, *26*, 1215–1227.
- Salat, D. H., Tuch, D. S., Hevelone, N. D., Fischl, B., Corkin, S., Rosas, H. D., et al. (2005). Age-related changes in prefrontal white matter measured by diffusion tensor imaging. *Annals of the New York Academy of Sciences*, *1064*, 37–49.
- Salthouse, T. A. (1992a). *Mechanisms of age-cognition relations in adulthood*. Hillsdale, NJ: Erlbaum.
- Salthouse, T. A. (1992b). What do adult age differences in the Digit Symbol Substitution Test reflect? *Journal of Gerontology*, *47*, P121–P128.
- Salthouse, T. A., Atkinson, T. M., & Berish, D. E. (2003). Executive functioning as a potential mediator of age-related cognitive decline in normal adults. *Journal of Experimental Psychology: General*, *132*, 566–594.
- Schmahmann, J. D., & Pandya, D. N. (2006). *Fiber pathways of the brain*. New York: Oxford University Press.
- Schulte, T., Sullivan, E. V., Muller-Oehring, E. M., Adalsteinsson, E., & Pfefferbaum, A. (2005). Corpus callosal microstructural integrity influences interhemispheric processing: A diffusion tensor imaging study. *Cerebral Cortex*, *15*, 1384–1392.
- Sohn, M. H., Ursu, S., Anderson, J. R., Stenger, V. A., & Carter, C. S. (2000). Inaugural article: The role of prefrontal cortex and posterior parietal cortex in task switching. *Proceedings of the National Academy of Sciences, U.S.A.*, *97*, 13448–13453.
- Song, A. W., Wong, E. C., Tan, S. G., & Hyde, J. S. (1996). Diffusion weighted fMRI at 1.5 T. *Magnetic Resonance in Medicine*, *35*, 155–158.
- Song, S. K., Sun, S. W., Ju, W. K., Lin, S. J., Cross, A. H., & Neufeld, A. H. (2003). Diffusion tensor imaging detects and differentiates axon and myelin degeneration in mouse optic nerve after retinal ischemia. *Neuroimage*, *20*, 1714–1722.
- Song, S. K., Sun, S. W., Ramsbottom, M. J., Chang, C., Russell, J., & Cross, A. H. (2002). Dysmyelination revealed through MRI as increased radial (but unchanged axial) diffusion of water. *Neuroimage*, *17*, 1429–1436.
- Spaniol, J., Madden, D. J., & Voss, A. (2006). A diffusion model analysis of adult age differences in episodic and semantic long-term memory retrieval. *Journal of Experimental Psychology: Learning, Memory, and Cognition*, *32*, 101–117.
- Sullivan, E. V., Adalsteinsson, E., Hedehus, M., Ju, C., Moseley, M., Lim, K. O., et al. (2001). Equivalent disruption of regional white matter microstructure in ageing healthy men and women. *NeuroReport*, *12*, 99–104.
- Sullivan, E. V., Adalsteinsson, E., & Pfefferbaum, A. (2006). Selective age-related degradation of anterior callosal fiber bundles quantified in vivo with fiber tracking. *Cerebral Cortex*, *16*, 1030–1039.
- Sullivan, E. V., & Pfefferbaum, A. (2006). Diffusion tensor imaging and aging. *Neuroscience and Biobehavioral Reviews*, *30*, 749–761.
- Sun, S. W., Liang, H. F., Le, T. Q., Armstrong, R. C., Cross, A. H., & Song, S. K. (2006). Differential sensitivity of in vivo and ex vivo diffusion tensor imaging to evolving optic nerve injury in mice with retinal ischemia. *Neuroimage*, *32*, 1195–1204.

- Tisserand, D. J., & Jolles, J. (2003). On the involvement of prefrontal networks in cognitive ageing. *Cortex*, *39*, 1107–1128.
- Tisserand, D. J., Pruessner, J. C., Sanz Arigita, E. J., van Boxtel, M. P., Evans, A. C., Jolles, J., et al. (2002). Regional frontal cortical volumes decrease differentially in aging: An MRI study to compare volumetric approaches and voxel-based morphometry. *Neuroimage*, *17*, 657–669.
- Verhaeghen, P., & Cerella, J. (2002). Aging, executive control, and attention: A review of meta-analyses. *Neuroscience and Biobehavioral Reviews*, *26*, 849–857.
- Visscher, K. M., Miezin, F. M., Kelly, J. E., Buckner, R. L., Donaldson, D. I., McAvoy, M. P., et al. (2003). Mixed blocked/event-related designs separate transient and sustained activity in fMRI. *Neuroimage*, *19*, 1694–1708.
- Wagenmakers, E.-J., van der Maas, H. L. J., & Grasman, R. P. P. (2007). An EZ-diffusion model for response time and accuracy. *Psychonomic Bulletin & Review*, *14*, 3–22.
- Wechsler, D. (1981). *Wechsler Adult Intelligence Scale—revised*. New York: Psychological Corporation.
- Yushkevich, P. A., Piven, J., Hazlett, H. C., Smith, R. G., Ho, S., Gee, J. C., et al. (2006). User-guided 3D active contour segmentation of anatomical structures: Significantly improved efficiency and reliability. *Neuroimage*, *31*, 1116–1128.